4

Basic Principles of MR Image Formation

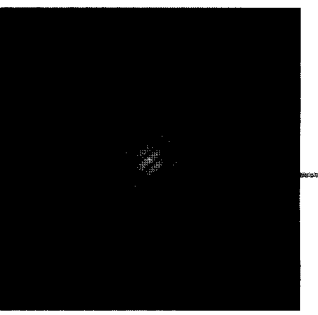

Introduction

As its name implies, the goal of magnetic resonance imaging is the formation of an image. It is important to recognize, however, that in the context of MRI, an **image** is not a photograph of the object being scanned, but rather it is a map that depicts the spatial distribution of some property related to the spins within the sample. Those properties might reflect the density of the spins, their mobility, or the T_1 or T_2 relaxation times for the tissues in which the spins reside. For example, T_1-weighted images depict the spatial distribution of T_1 values, so that voxels with short T_1 values are bright and voxels with long T_1 values are dark. Similarly, T_2^* images, as used in BOLD-contrast fMRI, are brighter where T_2^* values are long and darker where T_2^* values are short. Images can also be constructed that depict the spatial distribution of statistical properties, such as the difference between two experimental conditions. We will return to the construction of this type of image in Chapter 12.

While creating an image from MR signal may seem to be trivial or commonplace, remember from Chapter 1 that more than 25 years passed between the first NMR experiment (1945) and the first MR image (1972). Indeed, during that period, researchers actively strove to make their samples as homogeneous as possible so that no spatial variability could corrupt the data. Remember also that the 2003 Nobel Prize in Physiology or Medicine was awarded not for the discovery of medical applications of magnetic resonance, but instead for the development of techniques for image formation. In this chapter, we describe the fundamental concepts of image formation by illustrating how spatial information is encoded and decoded by MRI scanners. Specific topics include slice excitation, frequency encoding, phase encoding, and the representation of MRI data in *k*-space.

The fundamental concept underlying image formation in MRI is that of the magnetic gradient, or spatially varying magnetic field. In the first MRI experiments conducted by Purcell, Bloch, and other early researchers, the magnetic fields used were uniform, so that all spins in the entire sample experienced the same magnetic field. But as Lauterbur later demonstrated, superimposition of a second magnetic field that varies linearly across space will cause spins at different locations to precess at different frequencies in a controlled fashion. By measuring changes in magnetization as a function of

image A visual description of how one or more quantities vary over space.

Larmor frequency The resonant frequency of a spin within a magnetic field of a given strength. It defines the frequency of electromagnetic radiation needed during excitation to make spins change to a high-energy state, as well as the frequency emitted by spins when they return to the low-energy state.

B The sum of all magnetic fields experienced by a spin.

Bloch equation An equation that describes how the net magnetization of a spin system changes over time in the presence of a time-varying magnetic field.

spatial gradient (G) A magnetic field whose strength varies systematically over space. Note that since a given spatial location only experiences one magnetic field, which represents the sum of all fields present, spatial gradients in MRI act to change the effective strength of the main magnetic field over space.

precession frequency, the total MR signal can be parsed into components associated with different frequencies. We will thus begin this chapter by analyzing MR signal using the Bloch equation and by discussing the influence of magnetic gradients upon the MR signal.

Analysis of MR Signal

Recall that the precession frequency of a spin within a magnetic field (i.e., the **Larmor frequency**) is determined by two factors: the gyromagnetic ratio, which is a constant for a given atomic nucleus, and the magnetic field strength (see Equation 3.14). Likewise, the net magnetization of a spin system precesses around the main field axis at the Larmor frequency when tipped toward the transverse plane (see Equation 3.28). Since the Larmor frequency depends upon the strength of the magnetic field, changes in the strength of the magnetic field will also change the Larmor frequency. Keep in mind that during MR imaging, a spin experiences only one magnetic field, **B**, which represents the sum of all magnetic fields at its location.

In the previous chapter, we described two types of magnetic fields that are important for the generation of MR signal: the static (or main) field, $\mathbf{B_0}$, and the electromagnetic (or radiofrequency) field, $\mathbf{B_1}$. The static magnetic field aligns the precession axes of the nuclei and generates the net magnetization, **M**, and the electromagnetic field excites the net magnetization so that it can be measured in detector coils. The combined effects of these fields upon the net magnetization of a spin system were described by the **Bloch equation** (see Equation 3.47). We now introduce a third kind of magnetic field, the **spatial gradient, G,** which alters the precession frequencies of spins dependent upon their spatial location. With the addition of gradient fields as a component of **B**, we will solve the Bloch equation to account for all external magnetic fields, including gradient fields that vary over space. This will allow us to understand the strategies used for image formation. We repeat the Bloch equation here as Equation 4.1 for ease of reference:

$$\underbrace{\frac{d\mathbf{M}}{dt}}_{\text{Change in magnetization over time}} = \underbrace{\gamma \mathbf{M} \times \mathbf{B}}_{\text{Precession term}} + \underbrace{\frac{1}{T_1}(\mathbf{M}_o - \mathbf{M}_z)}_{T_1 \text{ term}} - \underbrace{\frac{1}{T_2}(\mathbf{M}_x + \mathbf{M}_y)}_{T_2 \text{ term}} \qquad [4.1]$$

The Bloch equation describes the change in net magnetization as the sum of three terms. As given by the precession term, the MR signal precesses around the main axis of the magnetic field at a rate given by the gyromagnetic ratio and the field strength (see Figure 3.11). The T_1 term indicates that the longitudinal component of the net magnetization recovers at a rate given by T_1 (see Figure 3.18A), and the T_2 term indicates that the transverse component of the net magnetization decays at a rate given by T_2 (see Figure 3.18B). Remember that in MR, the term *longitudinal* refers to the axis parallel to the main magnetic field and the term *transverse* refers to the plane perpendicular to the main magnetic field.

We will next attempt to solve the Bloch equation to determine the MR signal at each point in time, $M(t)$. First we break down the Bloch equation, which describes the MR signal in a three-dimensional vector format, into a simplified scalar form along each axis. Figure 4.1 illustrates that the net magnetization vector can be thought of either as a single vector in three dimen-

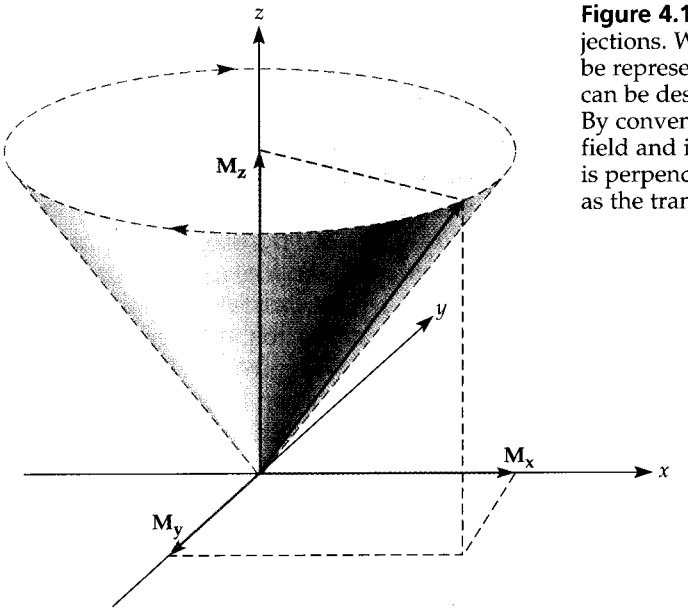

Figure 4.1 The net magnetization vector and its axis projections. While the net magnetization, **M**, of a sample can be represented as a single vector (shown in blue), it also can be described by a set of three vectors: $\mathbf{M}_x$, $\mathbf{M}_y$, and $\mathbf{M}_z$. By convention, the z-axis is parallel to the main magnetic field and is known as the longitudinal axis. The x–y plane is perpendicular to the main magnetic field and is known as the transverse plane.

sions or as a set of three vectors along each of the three cardinal axes. To represent the Bloch equation in scalar form, we need to isolate changes along each axis. Note that the behavior of the net magnetization in the x- and y-axes depends on both the precession term and the T_2 term. In contrast, the change in magnetization in the z-axis depends only on the T_1 term. Considering the axes separately, we can rearrange Equation 4.1:

$$\frac{dM_x}{dt} = \gamma M_y B - \frac{M_x}{T_2} \qquad [4.2a]$$

$$\frac{dM_y}{dt} = -\gamma M_x B - \frac{M_y}{T_2} \qquad [4.2b]$$

$$\frac{dM_z}{dt} = -\gamma \frac{(M_z - M_0)}{T_1} \qquad [4.2c]$$

So, Equations 4.2a and 4.2b describe the changes in the x- and y-directions of the magnetization over time, as the spin precesses about the main axis. The time constant T_2 specifies the rate of decay of magnetization in the transverse plane defined by the x- and y-axes, but it has no effect upon the longitudinal magnetization along the z-axis. Equation 4.2c describes the change in the longitudinal magnetization over time, as it recovers at a rate specified by T_1.

Longitudinal Magnetization (M_z)

The longitudinal magnetization depends only on a single equation (4.2c), which is a first-order ordinary differential equation. Thus, its solution is an exponential recovery function that describes the return of the main magnetization to the original state. Equation 4.3 replaces dM_z/dt with a mathematical equivalent, $d(M_z - M_0)/dt$, that represents the change in longitudinal magnetization from the fully relaxed state, M_0:

$$\frac{d(M_z - M_0)}{dt} = -\frac{M_z - M_0}{T_1} \qquad [4.3]$$

Swapping sides for dt and $M_z - M_0$, we get:

$$\frac{d(M_z - M_0)}{M_z - M_0} = -\frac{dt}{T_1} \qquad [4.4]$$

By integrating both sides of this equation, we obtain Equation 4.5. This equation states that the natural log of the change in longitudinal magnetization over time (0 to t') is equal to the change in time divided by the constant T_1:

$$ln[M_z(t) - M_0]\Big|_0^{t'} = -\frac{t}{T_1}\Big|_0^{t'} \qquad [4.5]$$

If we assume that the initial magnetization at time zero is given by M_{z0}, the solution for M_z at a later time point (t) is given by Equation 4.6. This equation states that the longitudinal magnetization (M_z) is equal to the fully relaxed magnetization, plus the difference between the initial and fully relaxed magnetization states, multiplied by an exponential time constant. Note that since M_{z0} is always less than M_0, the exponential term describes how much longitudinal magnetization is lost at a given point in time. As t increases, more longitudinal magnetization is recovered and the signal M_z approaches the fully relaxed signal M_0:

$$M_z = M_0 + (M_{z0} - M_0)e^{-t/T_1} \qquad [4.6]$$

To illustrate T_1 recovery, let us consider some extreme values for the initial magnetization, M_{z0}. Consider when the net magnetization is fully relaxed (Figure 4.2A). Here, M_{z0} is equal to M_0, and the term $(M_{z0} - M_0)$ will therefore be zero. Once the net magnetization is fully relaxed, it does not change over time, as indicated by the horizontal line segment. However, after an excitation pulse is applied (Figure 4.2B), the net magnetization is tipped entirely into the transverse plane and the net longitudinal magnetization is zero. The subsequent recovery of longitudinal magnetization is given by:

$$M_z = M_0(1 - e^{-t/T_1}) \qquad [4.7]$$

as shown in Figure 4.2C. This equation is important for determining the imaging parameters for T_1-contrast images. For example, by choosing when to acquire an image, we can make that image more or less sensitive to T_1 dif-

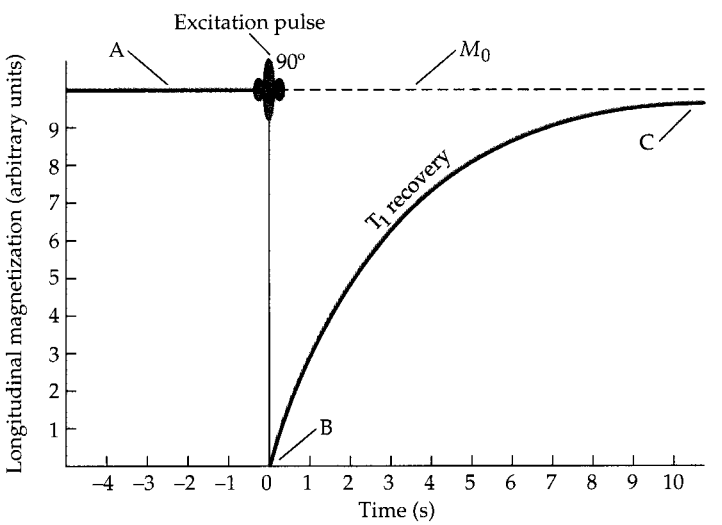

Figure 4.2 The change in longitudinal magnetization over time is known as T_1 recovery. When fully recovered (A), the longitudinal magnetization is at its maximum value, as shown by the dotted line, and does not change over time. However, following an excitation pulse that tips the net magnetization into the transverse plane, there will be zero longitudinal magnetization (B). As time passes following excitation, the longitudinal magnetization recovers toward its maximum value (C). The time constant T_1 governs this recovery process.

ferences between tissues. The details of pulse sequences used for T_1 contrast generation are further discussed in Chapter 5.

Solution for Transverse Magnetization (M_{xy})

The solution for the transverse magnetization is complicated by the fact that we must now consider the plane defined by two axes, x and y. Equations 4.2a and 4.2b reorganize the Bloch equation, treating the precession term as one-dimensional projections along the x- and y-axes of an object undergoing circular motion and the T_2 term as a decay factor (Figure 4.3). Solving for M_x and M_y, given an initial magnetization of $(-M_0, 0)$, we get the following equation pair:

$$M_x = (-M_0 \cos \omega t)e^{-t/T_2} \quad [4.8a]$$

$$M_y = (M_0 \sin \omega t)e^{-t/T_2} \quad [4.8b]$$

Though these equations appear complex, each describes two components that are illustrated in Figure 4.3. The parenthetical term (e.g., $M_0 \cos \omega t$) describes a one-dimensional projection of circular motion with constant velocity. The exponential term (i.e., e^{-t/T_2}) describes the decay of the circle over time. Together, they form an inward spiral pattern. As time (t) increases, the transverse magnetization will spiral farther inward and more and more transverse signal will be lost. The constant T_2 determines the rate at which the

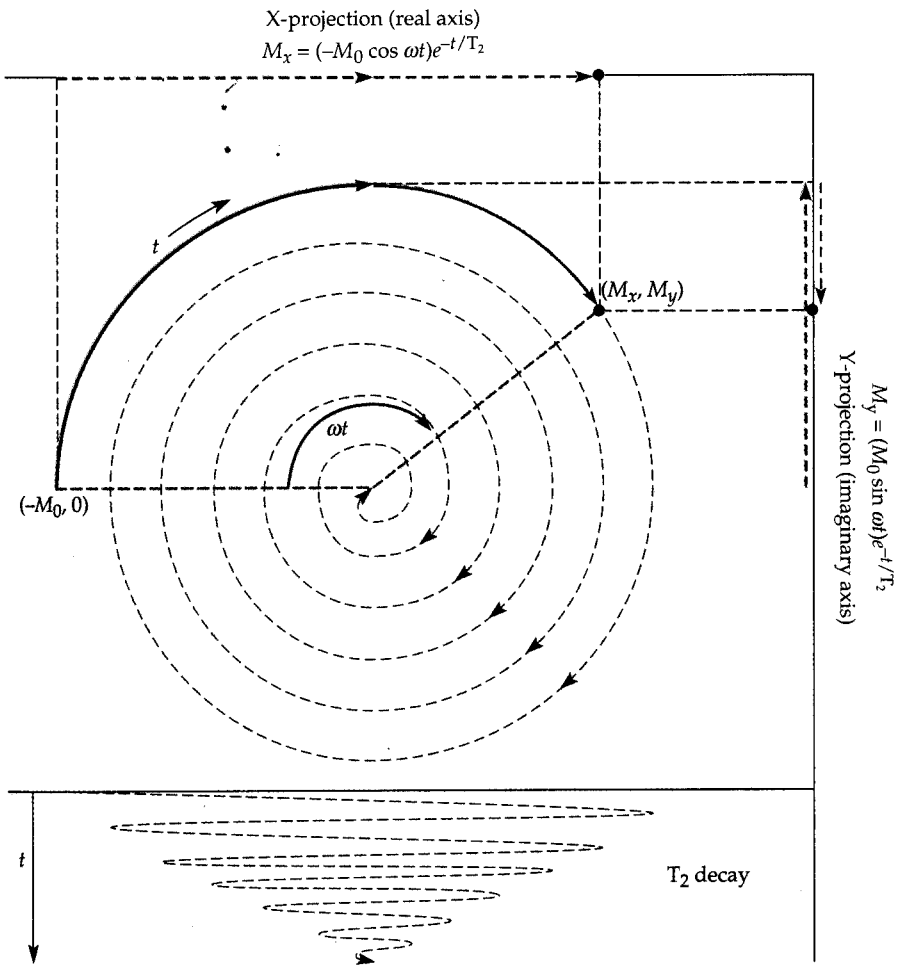

Figure 4.3 The change in transverse magnetization over time (t). The magnetism in the transverse plane is a vector defined by its angle and magnitude. As time passes, its angle follows a circular motion with constant angular velocity ω, while its magnitude decays with time constant T_2. These two components combine to form the inward spiral path shown (dashed lines). Shown at the top and right sides of the spiral path are its projections onto the x- and y-axes, respectively. Within each axis, the projection of the transverse magnetization is a one-dimensional oscillation, as illustrated by the blue and green lines. This oscillation is shown over time at the bottom of the figure, which illustrates the decaying MR signal.

phase Accumulated change in angle.

spiral shrinks. The quantity ωt is the angle of the net magnetization within the transverse plane and thus determines how fast the spiral turns.

We can combine the x- and y-components of the net magnetization into a more generalized single quantity, M_{xy}, which represents the transverse magnetization. The quantity M_{xy} is traditionally represented as a complex number, with one dimension represented using a real component and another represented using an imaginary component (Equation 4.9). The distinction between real and imaginary components will be very useful for the discussion of image formation later in this chapter.

$$M_{xy} = M_x + iM_y = -M_0(\cos \omega t - i \sin \omega t)\, e^{-t/T_2} \qquad [4.9]$$

This equation depends on a specific initial condition for (M_x, M_y) at $(-M_0, 0)$. For an arbitrary initial magnitude of the transverse magnetization $M_{xy0} = M_{x0} + iM_{y0}$, the transverse magnetization can be represented as:

$$M_{xy} = M_{xy0}\, e^{-t/T_2} e^{-i\omega t} \qquad [4.10]$$

Here we use the term, $e^{-i\omega t}$, which is identical to the term, $(\cos \omega t - i \sin \omega t)$, from Equation 4.9, to simplify the later derivation of the MR signal equation. The solution shown in Equation 4.10 states that the transverse magnetization depends upon three factors: the initial magnitude of the transverse magnetization (M_{xy0}), a loss of transverse magnetization over time due to T_2 effects (e^{-t/T_2}), and the accumulated **phase** ($e^{-i\omega t}$). Note that at $t = 0$, the exponential terms e^{-t/T_2} and $e^{-i\omega t}$ both reduce to $e^0 = 1$, so that the transverse magnetization is given by M_{xy0}. But after a long period of time (i.e., $t = \infty$), the term e^{-t/T_2} will become exceedingly small, and thus the transverse MR signal will be zero. Thus, Equation 4.10 is important for determining the imaging parameters for T_2-contrast images. As with T_1, by choosing when to acquire an image, we can make that image more or less sensitive to T_2 differences between tissues. To obtain contrast based upon the T_2 relaxation parameter, an intermediate time of image acquisition must be chosen, as will be discussed in the next chapter. The decay of the transverse magnetization, visualized in one dimension, is illustrated at the bottom of Figure 4.3. The details of pulse sequences used for T_2 contrast generation will be further discussed in Chapter 5.

Thought Question

Why does the transverse magnetization vector take a spiraling path rather than a circular path? How does the amplitude of the measured MR signal change over time?

Now (after the spin excitation), the magnetic field, **B**, experienced by spins at a given spatial location depends upon both the large static field, $\mathbf{B_0}$, and the smaller gradient field, **G**. The static field is oriented along the main axis of the scanner, and the gradient field modulates the strength of the main static field along the x-, y-, and z-axes. Note that while the magnitude of **B** varies depending upon the spatial location (x, y, z), its direction is always pointing along the main field. Therefore, we can describe the magnitude of the total magnetic field, **B**, experienced by a spin system at a given spatial location (x, y, z) and time point (t) as a linear combination of the static field and direction-specific time-varying gradient fields:

$$B(t) = B_0 + G_x(t)x + G_y(t)y + G_z(t)z \qquad [4.11]$$

Knowing that $\omega = \gamma B$, we can substitute the ω term in Equation 4.10 using the magnitude of the total magnetic field described in Equation 4.11 and get the following rather intimidating equation. Here we have split the exponential $e^{-i\omega t}$ into separate terms that describe the accumulated phase caused by the strength of the static magnetic field (B_0) and by the time-varying gradient fields ($G_x(t)$, $G_y(t)$, $G_z(t)$):

$$M_{xy}(x,y,z,t) = M_{xy0}(x,y,z)e^{-t/T_2}e^{-i\gamma B_0 t}e^{-i\gamma\int_0^t (G_x(t)x+G_y(t)y+G_z(t)z)dt} \quad [4.12]$$

Again, although this equation has many components and seems complex, it can be broken down into simpler and more understandable parts. It states that the transverse magnetization for a given spatial location and time point, $M_{xy}(x, y, z, t)$, is governed by four factors: (1) the original magnetization at that spatial location, $M_{xy0}(x, y, z)$; (2) the signal loss due to T_2 effects, e^{-t/T_2}; (3) the accumulated phase due to the main magnetic field, $e^{-i\gamma B_0 t}$; and (4) the accumulated phase due to the gradient fields:

$$e^{-i\gamma\int_0^t (G_x(t)x+G_y(t)y+G_z(t)z)dt}$$

Note that this last factor is indicated as an integral over time because gradients may change over time in some forms of MRI. If a constant gradient along one direction were used (e.g., G along the x-direction), the accumulated phase it causes could be more simply described as $\gamma G_x t$.

Let us pause for a moment to review what we have learned so far. We know that the net magnetization of a sample within a magnetic field can be thought of as a vector with magnitude and direction. The net magnetization vector can be broken down into longitudinal (along the static magnetic field) and transverse (perpendicular to the static magnetic field) components. After the net magnetization is tipped toward the transverse plane by an excitation pulse, it precesses around the longitudinal axis at the Larmor frequency. The precession of the net magnetization in the transverse plane allows measurement of MR signal. We also have just learned that the introduction of a spatial magnetic gradient alters the transverse magnetization over time because the frequency of precession depends upon the local magnetic field strength. This last point suggests that spatial gradients may allow encoding of spatial information within the MR signal. We explore this possibility in the next section.

The MR Signal Equation

MRI does not use separate receiving antennae for individual voxels. Indeed, such a setup would be impossible given that there may be 100,000 or more voxels within a single imaging volume. We use instead a single antenna (e.g., a volume coil) that covers a large region. The **MR signal** measured by the antenna reflects the sum of the transverse magnetizations of all voxels within the excited sample. We emphasize this important point because it underlies all of the principles of image formation discussed later in this chapter: The total signal measured in MRI combines the changes in net magnetization generated at every excited voxel. This can be restated in the formal mathematical terms of Equation 4.13, which expresses the MR signal at a given point in time, $S(t)$, as the spatial summation of the MR signal from every voxel:

$$S(t) = \int_x \int_y \int_z M_{xy}(x, y, z, t)dx\, dy\, dz \quad [4.13]$$

MR signal The current measured in a detector coil following excitation and reception.

MR signal equation A single equation that describes the obtained MR signal as a function of the properties of the object being imaged under a spatially varying magnetic field.

slice A single slab of an imaging volume. A slice has thickness defined by the strength of the gradient and the bandwidth of the electromagnetic pulse used to select it.

Combining Equations 4.12 and 4.13 results in Equation 4.14:

$$S(t)=\int_x \int_y \int_z M_{xy0}(x,y,z)e^{-t/T_2}e^{-iw_0t}e^{-i\gamma\int_0^t (G_x(t)x+G_y(t)y+G_z(t)z)dt}dx\,dy\,dz \quad [4.14]$$

Equation 4.14 can be read as stating that the total MR signal measured at any point in time reflects the sum across all voxels of the net magnetization at time point zero, multiplied by a decay factor based upon T_2, with accumulated phase given by the strength of the static magnetic field and of the gradient field at that point in space. This vastly important equation is known as the **MR signal equation,** because it reveals the relationship between the acquired signal, $S(t)$, and the properties of the object being imaged, $M(x,y,z)$. It is important to recognize that this equation is sufficiently general to describe the MR signal in virtually all imaging methods.

In practice, the term $e^{-i\omega_0 t}$ is not necessary for calculation of MR signal, because modern MRI scanners demodulate the detected signal with the resonance frequency ω_0. That is, they synchronize data acquisition to the resonance frequency. This demodulation process is analogous to the idea of transformation from laboratory to rotating reference frames, as introduced in Chapter 3. Imagine that you were watching the precession of the transverse magnetization from the laboratory (i.e., normal) reference frame. You would see the transverse magnetization spinning around the longitudinal axis at the Larmor frequency. Now imagine that you were rotating around the longitudinal axis at the same speed as the precessing magnetization. The magnetization vector would now appear to be still.

The T_2 decay term, e^{-t/T_2}, affects the magnitude of the signal but not its spatial location. Because it does not contain any spatial information, we can ignore it for the moment. By removing these two terms, we arrive at a simpler version of the MR signal equation:

$$S(t)=\int_x \int_y \int_z M_{xy0}(x,y,z)e^{-i\gamma\int_0^t (G_x(t)x+G_y(t)y+G_z(t)z)dt}dx\,dy\,dz \quad [4.15]$$

This equation illustrates the profound importance of the gradient fields for encoding spatial information within an MR image. In principle, we can collect a single MR image of an entire volume by systematically turning on gradient fields along x, y, and z. However, because three-dimensional (3-D) imaging sequences present additional technical challenges and are less tolerant of hardware imperfection, most forms of imaging relevant to fMRI studies use two-dimensional (2-D) imaging sequences. For the sake of simplicity, we will next discuss the principles underlying common 2-D imaging techniques. We will return to the less common 3-D imaging techniques at the end of this chapter.

Slice Selection, Spatial Encoding, and Image Reconstruction

Note that the simplified MR signal equation (see Equation 4.15) is still in 3-D form, in that the signal contribution from each spatial location depends upon all three spatial gradients. In order to reduce this signal equation to two dimensions, there must be some way to eliminate variation over one spatial dimension. This can be accomplished by separating the signal-acquisition process into two steps. First we select a particular **slice** within the total imaging volume using a one-dimensional excitation pulse. Then we use a two-dimensional encoding scheme within the slice to resolve the spatial distribution of the spin magnetizations. This two-step process forms the basis for most pulse sequences used in MRI, including those used for acquisition

of fMRI BOLD images. We will discuss the theoretical bases for these steps in this section, and describe their practical implementation in the following sections.

The basic concept of **slice selection** is the application of an electromagnetic pulse that excites spins within one slice but has no effect on spins outside the slice. The slice chosen by the selection process is defined by its location, orientation, and thickness. For example, let us assume that we want to create an image of a plane centered at $z = z_0$. For a given location (x, y) within that slice, the total magnetization summed along the z-direction, $M(x,y)$, for a thickness Δz is given by Equation 4.16. This equation describes the bulk magnetization of an individual voxel, or x–y coordinate pair, within the slice.

$$M(x,y) = \int_{z_0-\frac{\Delta z}{2}}^{z_0+\frac{\Delta z}{2}} M_{xy0}(x,y,z)dz \qquad [4.16]$$

Note that since we are integrating all signals along the z-direction, the magnetization, M, is dependent only on x and y, but not on z. Thus, by first selecting an imaging slice, the simplified MR signal equation (see Equation 4.15) can be further reduced into a 2-D form, as follows:

$$S(t) = \int_x \int_y M(x,y)e^{-i\gamma\int_0^t (Gx(\tau)x+Gy(\tau)y)d\tau}\,dx\,dy \qquad [4.17]$$

Equation 4.17 states that the total signal recorded from a slice depends upon the net magnetization at every (x, y) location within that slice, with the phase of individual voxels dependent upon the strength of the gradient fields at that location. Although the parts of Equation 4.17 are individually understandable, this equation is difficult to visualize and solve in its present form. To facilitate a better understanding of the relation between the MR signal, $S(t)$, and the object to be imaged, $M(x,y)$, MR researchers have adopted a different notation scheme known as ***k*-space.** Recognize that k-space differs in an important way from normal image space, in which the object resides. Consider the terms k_x and k_y in Equation 4.18. Each equation represents the time integral of the appropriate gradient multiplied by the gyromagnetic ratio:

$$k_x(t) = \frac{\gamma}{2\pi}\int_0^t G_x(\tau)d\tau \qquad [4.18a]$$

$$k_y(t) = \frac{\gamma}{2\pi}\int_0^t G_y(\tau)d\tau \qquad [4.18b]$$

These equations state that changes in k-space over time, or ***k*-space trajectories,** are given by the time integrals of the gradient waveforms. In other words, the k-space trajectories are simply the areas under the gradient waveforms, as illustrated in Figure 4.4 for a uniform gradient change over a time interval (t). By substituting these terms into Equation 4.17, we can restate the MR signal equation using k-space coordinates:

$$S(t) = \int_x \int_y M(x,y)e^{-i2\pi k_x(t)x}\,e^{-i2\pi k_y(t)y}dx\,dy \qquad [4.19]$$

Equation 4.19 is remarkable, because it indicates that k-space and image space have a straightforward relation: they are 2-D Fourier transforms of each other. Any signal that changes over time or space, no matter how complex, can be constructed from a series of simpler components in the frequency or spatial-frequency domain, respectively (Figure 4.5A–C). The

slice selection The combined use of a spatial magnetic field gradient and an electromagnetic pulse to excite spins within a slice.

***k*-space** A notation scheme used to describe MRI data. The use of k-space provides mathematical and conceptual advantages for describing the acquired MR signal in image form.

***k*-space trajectory** A path through k-space. Different pulse sequences adopt different k-space trajectories.

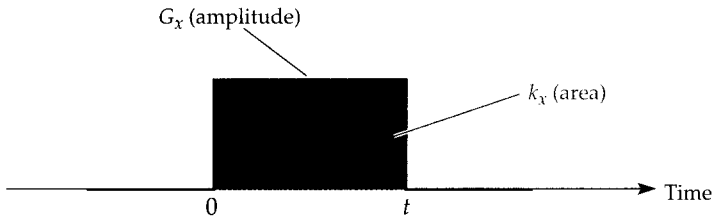

Figure 4.4 The relation between the gradient waveform and *k*-space. The effect of a gradient, G_x, upon a given voxel is expressed as the amplitude of the gradient signal over time. The change in *k*-space over time is given by the area under the square.

Fourier transform is one mathematical tool for this construction process. The mathematics of the Fourier transform are well established, so we can take advantage of those mathematics to decode the *k*-space representation of the MR signal, $S(t)$, into the magnetization at each spatial location, $M(x,y)$, creating a spatially informative image. Equation 4.19 suggests that an inverse Fourier transform can convert *k*-space data into an image, a process known

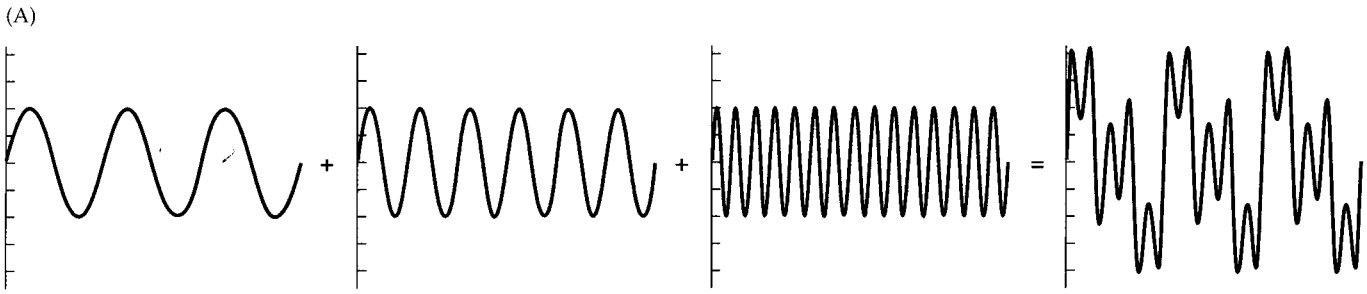

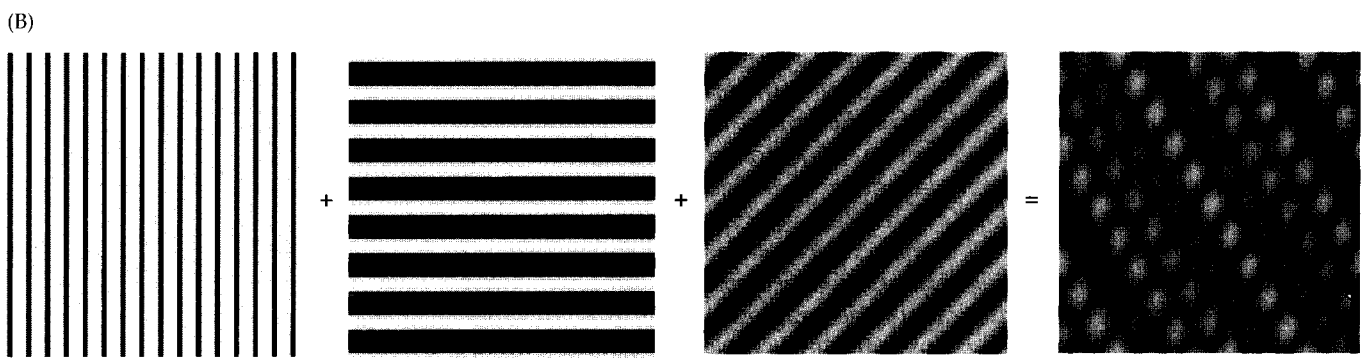

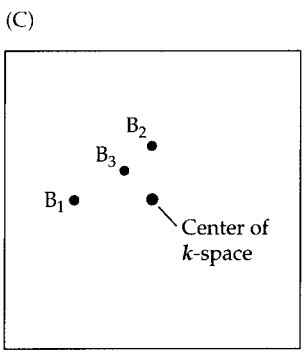

Figure 4.5 Constructing a complex waveform or image from simpler components. Any data, no matter how complex, can be constructed from simpler components. Shown in (A) are three sine waves, each with a different frequency. When combined, they form the waveform at right. By combining more and more sine waves of different frequencies and phases, very complex waveforms can be created, such as that of music. The same principle holds for two-dimensional data (B), except that here the components are gratings of particular spatial frequencies (i.e., how closely spaced are the bars), phases, and angles. By combining a very large number of these gratings, complex images can be created, such as those used in MRI. Shown in (C) is the *k*-space plot of the summed image; the individual gratings are associated with the three bright pixels.

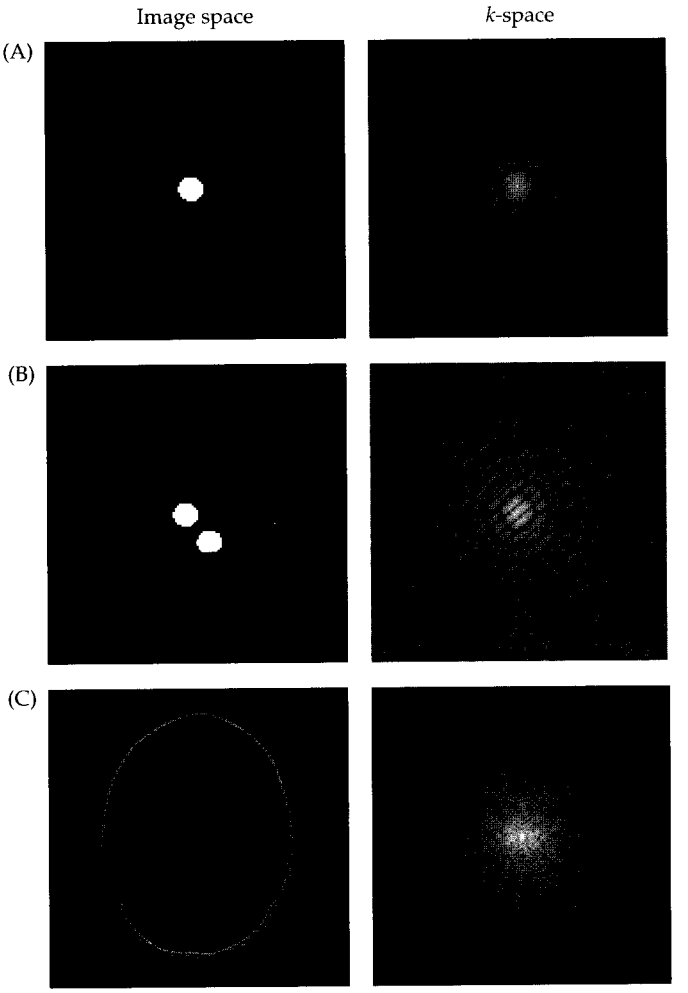

Figure 4.6 Images and their Fourier transforms. (A) A single circle at the center of the image space and the representation of the circle in *k*-space. Note that the *k*-space representation follows a sinc function, with greatest intensity at the center and intensity bands of decreasing amplitude toward the edges of the *k*-space. Addition of a second circle to the image space (B) introduces a grating pattern to the *k*-space. An image of the brain (C) contains much more spatial information, and thus its representation in *k*-space is similarly more complex.

as **image reconstruction.** Conversely, a forward Fourier transform can convert image-space data into *k*-space data.

To illustrate the relation between image space and *k*-space, Figure 4.6 shows some sample images and the resulting Fourier transforms. Think of each pair as showing an object and the acquired MR signal in its raw form within *k*-space. An image with a single circle at its center corresponds to a pattern of alternating light and dark circles throughout *k*-space (Figure 4.6A). As an aside, this pattern is equivalent to a 2-D Bessel sinc function. Note that the center of *k*-space represents the point in time when signal from all voxels is at the same phase, so it represents the total transverse magnetization within that slice. Thus, the center of *k*-space always has the highest signal of any point.

We can add a second circle to the image to illustrate another concept, that *k*-space reflects the **spatial frequency** of the object(s) in the image space. Spatial frequency defines how often some pattern occurs in space, just like temporal frequency (e.g., musical pitch) defines how often something occurs in time. Shown in Figure 4.6B are two circles, one offset from center. If we trace a line from the top left to the bottom right of the image, it will encounter two circles separated by a distance between their centers. The *k*-space data will thus have a spatial-frequency component along that line, with frequency equal to the inverse of that distance. This is visible as a grating running from top left to bottom right in the *k*-space image, on top of the concentric pattern that results from the shape of the circles.

image reconstruction The process by which raw MR signal, as acquired in *k*-space form, is converted into spatially informative images.

spatial frequency The frequency with which some pattern occurs over space.

Thought Question

How would the *k*-space data in Figure 4.6B change if the lower circle were moved to the bottom-left quadrant of the image? How would the *k*-space data change if it were moved farther toward the bottom-right corner?

Any image, no matter how complex, can be represented as an ensemble of spatial-frequency components. The *k*-space representation of an anatomical image is shown in Figure 4.6C. The *k*-space image is brightest in the center and darkest near the edges. This illustrates that low-spatial-frequency data from near the center of *k*-space is most important for determining the

signal-to-noise ratio of the image. In comparison, high-spatial-frequency data collected at the periphery of *k*-space helps to increase the spatial resolution of the image. Figure 4.7 illustrates this important distinction between the low-spatial-frequency and high-spatial-frequency regions of *k*-space. If from a normal photograph (Figure 4.7A) we take only the low-spatial-frequency region of its *k*-space data, the image would have most of the signal but would lack good spatial resolution (Figure 4.7B). But if we take only the high-spatial-frequency region of its *k*-space data, the image would have a low signal level but the spatial detail would be preserved (Figure 4.7C).

Contrary to intuition, there is *not* a one-to-one relation between points in *k*-space and voxels in image space. For an illustration of what each point in *k*-space represents, consider Figure 4.8. The center plot shows the *k*-space data (or raw MR signal). Each point in the *k*-space data is acquired at a different point in time and has contributions from all voxels within the slice. We have highlighted four sample *k*-space points, each showing the net magnetization vectors within each voxel (in image space) at the moment in time when that point in *k*-space was acquired. For the point at the center of *k*-space (Figure 4.8A), all of the magnetization vectors are at the same phase, and thus the total signal is at its maximum. At other *k*-space points (Figure 4.8B–D), the magnetization vectors differ across voxels, and the intensity of

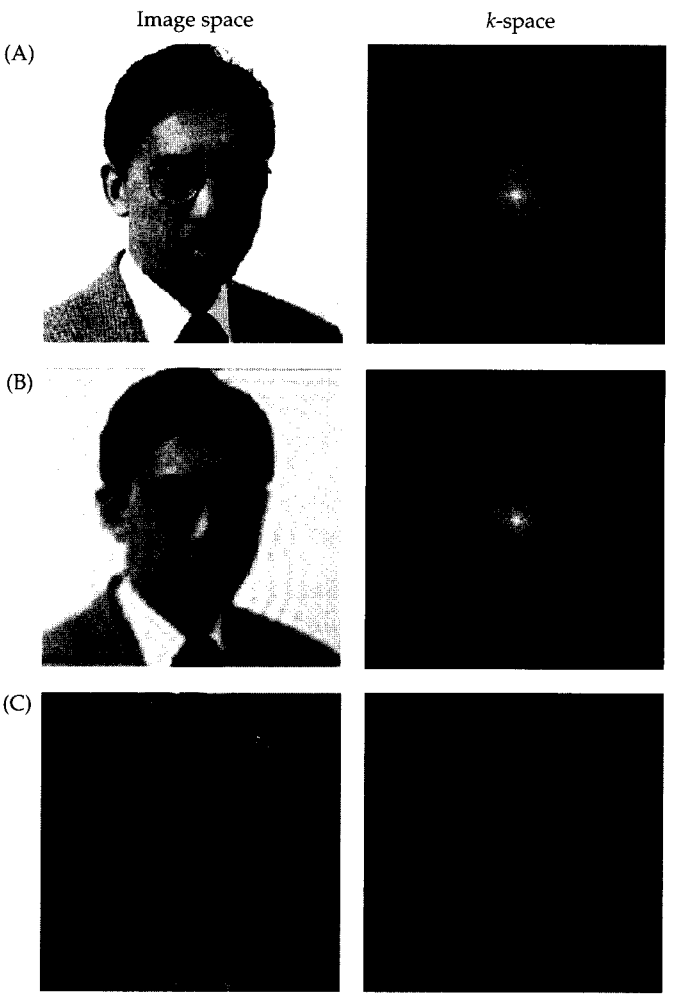

Figure 4.7 How different parts of *k*-space contribute to image space. Images such as this photograph of Dr. Seiji Ogawa can be converted using a Fourier transform into *k*-space data (A). Different parts of the *k*-space data correspond to different spatial-frequency components of the image. The center of *k*-space (B) provides low-spatial-frequency information, retaining most of the signal but not fine details. The periphery of *k*-space (C) provides high-spatial-frequency information, and thus image detail, but contributes relatively little signal to the image.

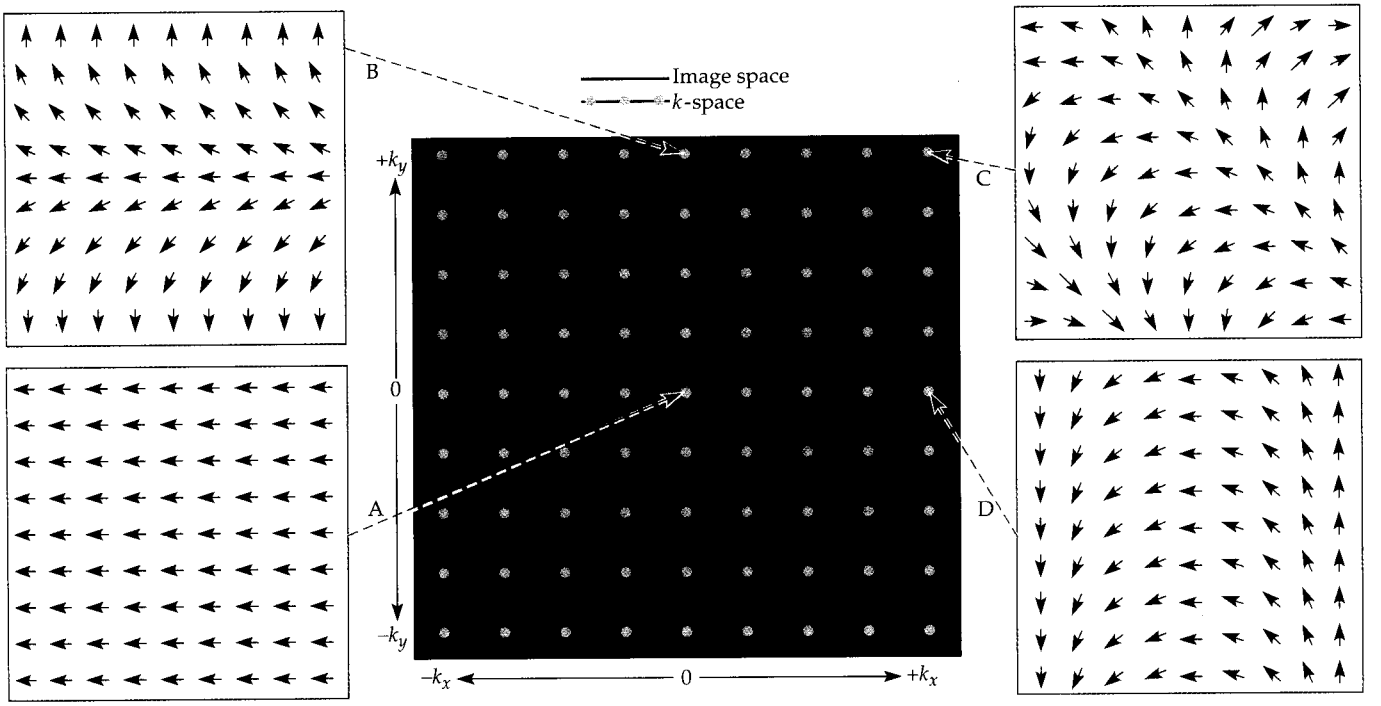

Figure 4.8 Contributions of different image locations to the raw *k*-space data. Each data point in *k*-space (shown in yellow) consists of the summation of MR signal from all voxels in image space under corresponding gradient fields. For four sample *k*-space points (A–D), the magnetization vectors across voxels in image space are illustrated. For the center of *k*-space, the phases for all voxels in the respective image space are identical (A), therefore leading to the maximum signal in *k*-space. For a data point where k_y is at the maximum and k_x is at zero (B), the phases of magnetization vectors in image space change rapidly along the *y*-direction but remain the same along the *x*-direction. For a data point where both k_x and k_y are large (C), the phases change rapidly along the combined diagonal direction. And finally, where k_y is zero and k_x is at its maximum (D), the phases change rapidly only along the *x*-direction.

the *k*-space point represents the sum of those vectors. In the section on 2-D spatial encoding, we will discuss how MR scanners adjust the spatial gradients over time to systematically sample all of these *k*-space points.

In summary, the process of 2-D image formation has the following stages shown in the flowchart below. First, the longitudinal magnetization of a single slice is tipped into the transverse plane by a process known as slice excitation. Next, the resulting transverse magnetization is encoded into two-dimensional raw data represented in *k*-space. Finally, the desired MR image is reconstructed using a two-dimensional inverse Fourier transform. We will discuss the practical implementation of these steps in the following sections.

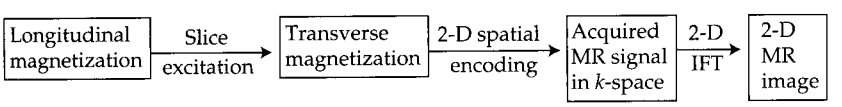

Slice Excitation

As indicated in the theoretical discussion in the previous section, the first step in an imaging sequence is slice selection. Remember that the goal of slice selection is to excite only a particular thin slab of the sample so that signal within that slab can be spatially encoded. From Chapter 3 we know that an electromagnetic field ($\mathbf{B}_1$) at the Larmor frequency, when applied in the transverse plane, tips the longitudinal magnetization. If the duration and

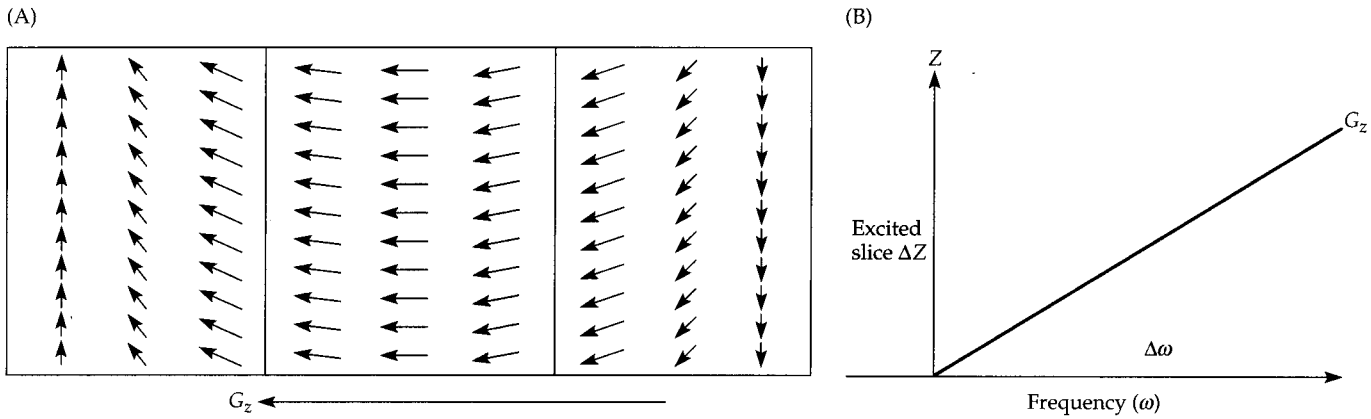

Figure 4.9 Slice selection. As shown in (A), application of a slice selection gradient (G_z) changes the Larmor frequency of spins within the sample. The gradient is chosen so that spins within the slice of interest (shading) will precess at the desired frequency. Following the application of the gradient, a subsequent excitation pulse at a given frequency (ω) and bandwidth ($\Delta\omega$) is applied. As shown in (B), the excitation frequency and frequency bandwidth determine the slice location (Z) and slice thickness (ΔZ).

interleaved slice acquisition The collection of data in an alternating order, so that data is first acquired from the odd-numbered slices and then from the even-numbered slices, to minimize the influence of excitation pulses upon adjacent slices.

strength of the electromagnetic field are appropriately calibrated, the longitudinal magnetization will rotate exactly into the transverse plane. Such a calibrated electromagnetic field is known as an excitation pulse. But if the magnetic field were uniform, the applied excitation pulse would affect all of the spins within the volume. However, by introducing a static gradient along the slice selection axis (e.g., G_z), we can tune the Larmor frequencies of all spins in the slice (and only spins in the slice) to match the frequency of the excitation pulse (Figure 4.9A and B).

Ideally, we would like to excite a perfectly rectangular slice along the z-direction; for example, we might excite all spins from $z = +10$ mm to $z = +15$ mm and no spins outside of that range. One might think that this could be achieved by a rectangular slice selection pulse, as shown in Figure 4.10A. However, a rectangular pulse actually contains a distribution of frequencies shaped like a sinc function, so it does not excite a rectangular slice. Instead, we must use a sinc-modulated electromagnetic pulse (Figure 4.10B). Since the Fourier transform of a sinc function is a rectangular function, a sinc-modulated pulse has a rectangular frequency response; thus it contains all frequencies within a band and no frequencies outside that band.

Although a perfectly rectangular slice profile would be optimal, it is difficult to achieve because of off-resonance excitation. As discussed in the previous chapter, off-resonance effects may excite spins to some intermediate stage, as they rotate about the $\mathbf{B}_{1\text{eff}}$ field. The primary consequence for fMRI is cross-slice excitation, or the bleeding of excitation from one slice to the next. If we excite adjacent slices sequentially (i.e., first, second, third, etc.), each slice will have been pre-excited by the previous excitation pulse, leading to saturation of the MR signal. To minimize this problem, most excitation schemes use **interleaved slice acquisition.** For example, if we are to excite ten contiguous slices, we will excite in order the first, third, fifth, seventh, ninth, second, fourth, sixth, eighth, and tenth slices. The use of interleaved slice acquisition effectively eliminates excitation overlap problems.

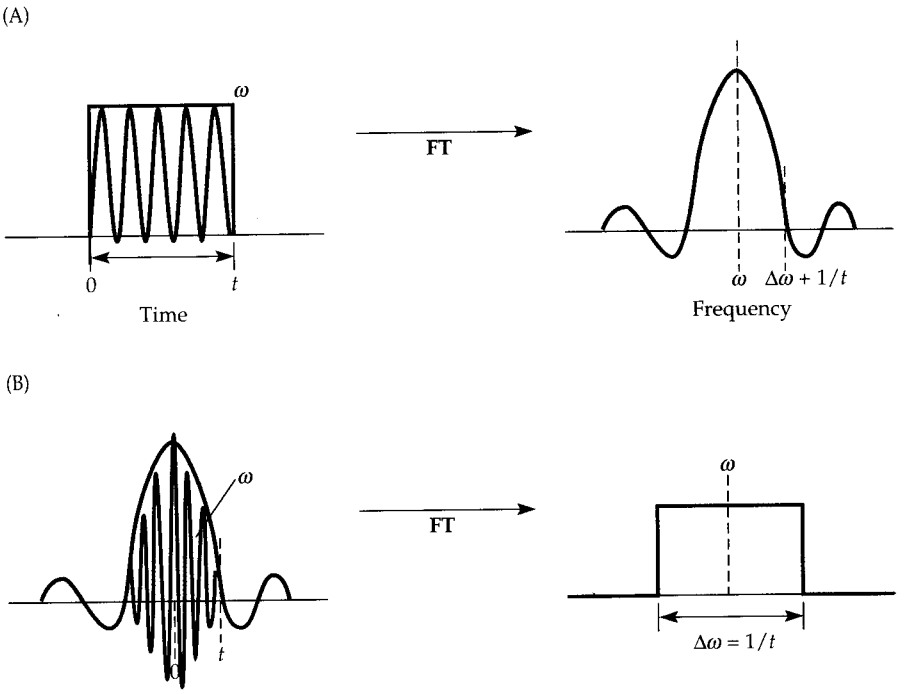

Figure 4.10 Possible slice selection pulses. (A) A rectangular slice selection pulse that consists of a constant application of a radiofrequency field at frequency ω_0 for a time t. The slice selection profile of this pulse is given by its Fourier transform (FT) and shown at right as a sinc function with fundamental frequency ω_0. This profile is not ideal for selection of a rectangular slice. However, (B) shows the use of a pulse with time amplitude given by a sinc function. This pulse gives a rectangular frequency profile and allows excitation of spins within a rectangular slice.

Slice location and thickness are determined by three factors: the center frequency of the excitation pulse (ω), the bandwidth of the excitation field ($\Delta\omega$), and the strength of the gradient field (G_z), as illustrated in Figure 4.11. Together, the center frequency and the gradient field determine the slice location, while the bandwidth and the gradient field determine the slice thickness. By sliding the center frequency up and down over successive acquisitions, MR signal from different slices can be selectively acquired. Likewise, by choosing a wide or narrow excitation bandwidth, thick or thin slices can be collected. Note that use of a stronger gradient, in principle, means that spins at nearby spatial locations will have greater differences in their Larmor frequencies, allowing more-selective excitation by a given electromagnetic pulse. Thus, stronger gradients increase spatial resolution across slices.

Thought Question

Assume that we doubled the strength of the gradient fields in our scanner. How would the frequency and bandwidth of the excitation pulse need to change to keep the same slice selection?

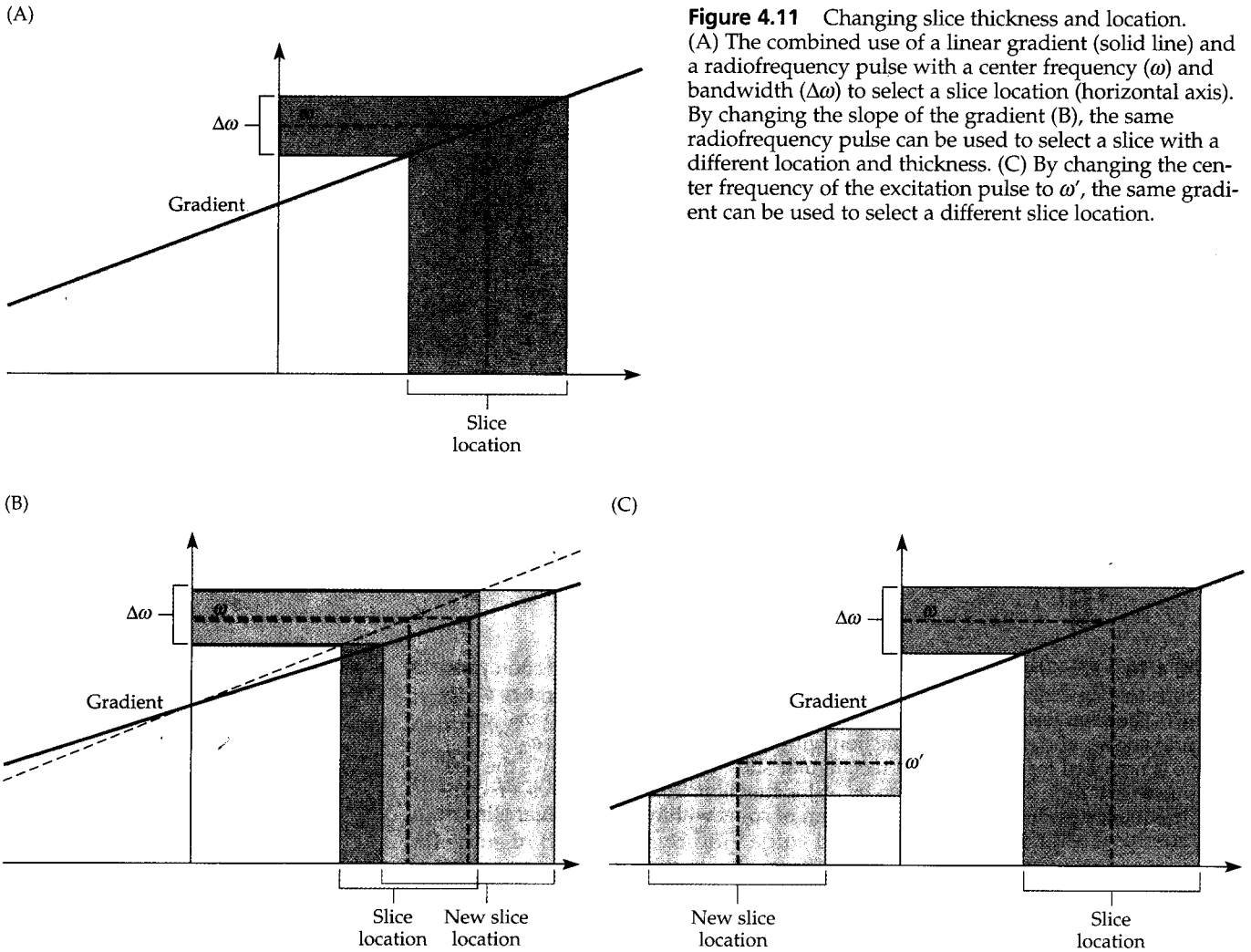

Figure 4.11 Changing slice thickness and location. (A) The combined use of a linear gradient (solid line) and a radiofrequency pulse with a center frequency (ω) and bandwidth ($\Delta\omega$) to select a slice location (horizontal axis). By changing the slope of the gradient (B), the same radiofrequency pulse can be used to select a slice with a different location and thickness. (C) By changing the center frequency of the excitation pulse to ω', the same gradient can be used to select a different slice location.

filling *k*-space The process of collecting samples from throughout *k*-space in order to collect data sufficient for image formation.

2-D Spatial Encoding

Once spins are excited within the desired slice, they can be spatially encoded so that MR signal from different parts of the image can be resolved. A unique frequency is assigned to all voxels within the slice, in a process known as frequency and phase encoding, to facilitate later reconstruction of the signal using the Fourier transform. To do this, a gradient magnetic field that differs across two dimensions (e.g., G_x, G_y) is applied to the sample. These gradients influence the individual spin phases for different voxels, as illustrated in Figure 4.12. To understand how the scanner hardware and software accomplish the encoding process, we must return to the concept of *k*-space. As we learned earlier in this chapter, if we reorganize signal $S(t)$ to $S(k_x(t), k_y(t))$ as indicated in Equation 4.19, then the MR signal can be represented by a 2-D function in a coordinate system where k_x and k_y are the two axes. This coordinate system defines *k*-space and has units in spatial frequency (1/distance). Because a complete sample of the *k*-space is usually required to construct an image, collecting the MR signal is often referred to as **filling *k*-space.**

Remember from Figure 4.4 that k_x and k_y are actually time integrals of the gradient waveform. Thus, by manipulating the gradient waveforms, we can

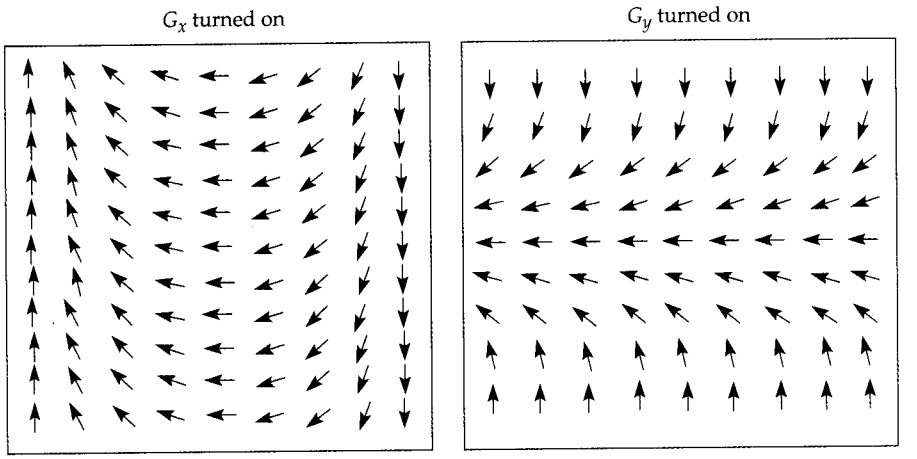

Figure 4.12 Effects of magnetic field gradients on spin phase. Application of magnetic field gradients influences the frequency of spins over space, and thus the accumulated phase over time. Shown are examples of gradients in the x- and y-directions.

control the sampling path within k-space during MR signal acquisition. For example, by altering the strength of different gradients over time, we could first collect data from the upper-left point in k-space, and then move rightward, and then downward, and then leftward, etc., tracing a snakelike path throughout the image. While any path that covers all of k-space can be used to collect the k-space data, in practice regular paths such as straight lines are preferred.

In typical anatomical imaging sequences (Figure 4.13A), k-space is filled one line at a time, following a succession of individual excitation pulses. During each excitation the combination of the electromagnetic pulse and the G_z gradient selects the desired slice. Then the G_y gradient is turned on before the data acquisition period, so that it accumulates a certain amount of phase offset before the activation of the G_x gradient. This results in the movement

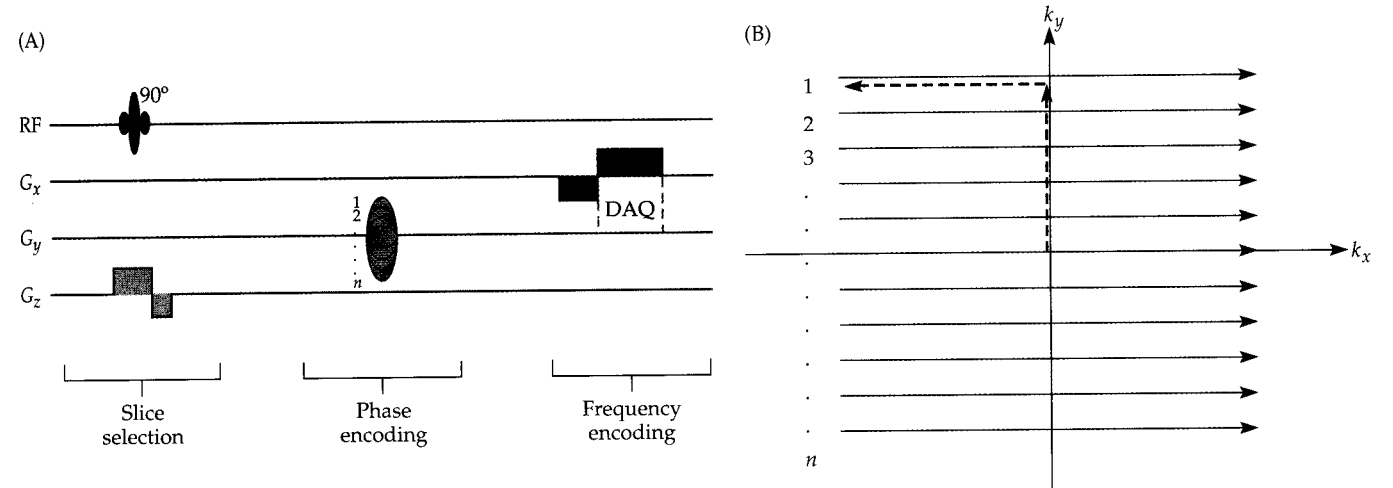

Figure 4.13 A typical two-dimensional gradient-echo pulse sequence. Shown in (A) are lines representing activity of the radiofrequency field (RF) and the three spatial gradients. The pulse sequence begins with a combined slice selection gradient (G_z) and excitation pulse. The G_y gradient is used for selecting one line of k-space following each excitation pulse, while the G_x gradient is turned on during data acquisition (DAQ). This sequence is known as a gradient-echo sequence, and it acquires each line of k-space following a separate excitation (B). Following n excitations, all of k-space is filled and image acquisition is complete.

phase-encoding gradient A gradient turned on before the data acquisition period, so that spins can accumulate differential phase offset over space.

frequency-encoding gradient A gradient turned on during the data acquisition period, so that the frequency of spin precession changes over space.

field of view (FOV) The total extent of an image along a spatial dimension.

of the effective location of data acquisition in *k*-space along the *y*-direction, as shown by the blue arrow in Figure 4.13B. In this example, G_y can be considered to be the **phase-encoding gradient.** During data acquisition, the G_x gradient is turned on, changing the frequency of the spins, so by convention G_x becomes the **frequency-encoding gradient.** Note, however, that both gradients act similarly in *k*-space, because k_x and k_y both reflect the time integrals of the gradient waveforms.

Recognize that *k*-space is sampled in a discrete fashion. Along the k_y direction, each line represents a separate amplitude of the G_y gradient (shown as 1...*n* steps in Figure 4.13). While the trajectory along the k_x direction is continuous, the MR signal is sampled digitally with a specific interval, so that each row consists of a number of discrete data points.

2-D Image Formation

After *k*-space is filled, a 2-D inverse Fourier transform is necessary for conversion of the raw data from *k*-space to image space, $M(x,y)$. It is important to recognize that the sampling parameters in these two spaces are inversely proportional to each other. In image space, the basic sampling unit is distance, while in *k*-space, the basic sampling unit is spatial frequency (1/distance). Qualitatively speaking, this means that a wider range of coverage in *k*-space results in higher spatial resolution in image space (i.e., smaller voxels). This concept can be appreciated by the photographs shown in Figure 4.7, which demonstrate that the periphery of *k*-space contributes to fine details of the image (i.e., spatial resolution). Conversely, finer sampling in *k*-space results in a greater extent of coverage, or a larger field of view, in the image domain. This relationship is illustrated graphically in Figure 4.14A–C and quantitatively in Equation 4.20a,b. Here, **field of view (FOV)** is defined as the total spatial extent along a dimension of image space (i.e., how large the image is). Typical fields of view in fMRI experiments are about 20 to 24 cm.

$$\mathrm{FOV}_x = \frac{1}{\Delta k_x} = \text{sampling rate along } k_x = \frac{1}{\frac{\gamma}{2\pi}(G_x \Delta t)} \qquad [4.20a]$$

$$\mathrm{FOV}_y = \frac{1}{\Delta k_y} = \text{sampling rate along } k_y = \frac{1}{\frac{\gamma}{2\pi}(\Delta G_y t)} \qquad [4.20b]$$

These equations can be reorganized (Equation 4.21a,b) to give the voxel size, which is just the FOV divided by the number of samples. Note that the quantities $2k_{x\max}$ and $2k_{y\max}$ refer to the total extent of *k*-space along each of the cardinal dimensions. If $k_{\max}$ is large, then the voxel size will be small.

$$\frac{\mathrm{FOV}_x}{M_x} = \frac{1}{M_x \Delta k_x} = \frac{1}{2k_{x\max}} \qquad [4.21a]$$

$$\frac{\mathrm{FOV}_x}{M_y} = \frac{1}{M_y \Delta k_y} = \frac{1}{2k_{y\max}} \qquad [4.21b]$$

In summary, the raw MR signal, $S(t)$, is a one-dimensional string of data points through *k*-space that has been sampled at a very high rate. This signal can be broken into two dimensions, according to k_x and k_y, to facilitate a 2-D inverse Fourier transform. Decreasing the separation between adjacent data points in *k*-space increases the FOV in image space. Likewise, increasing the extent of *k*-space decreases the voxel size in image space. Note also that if we

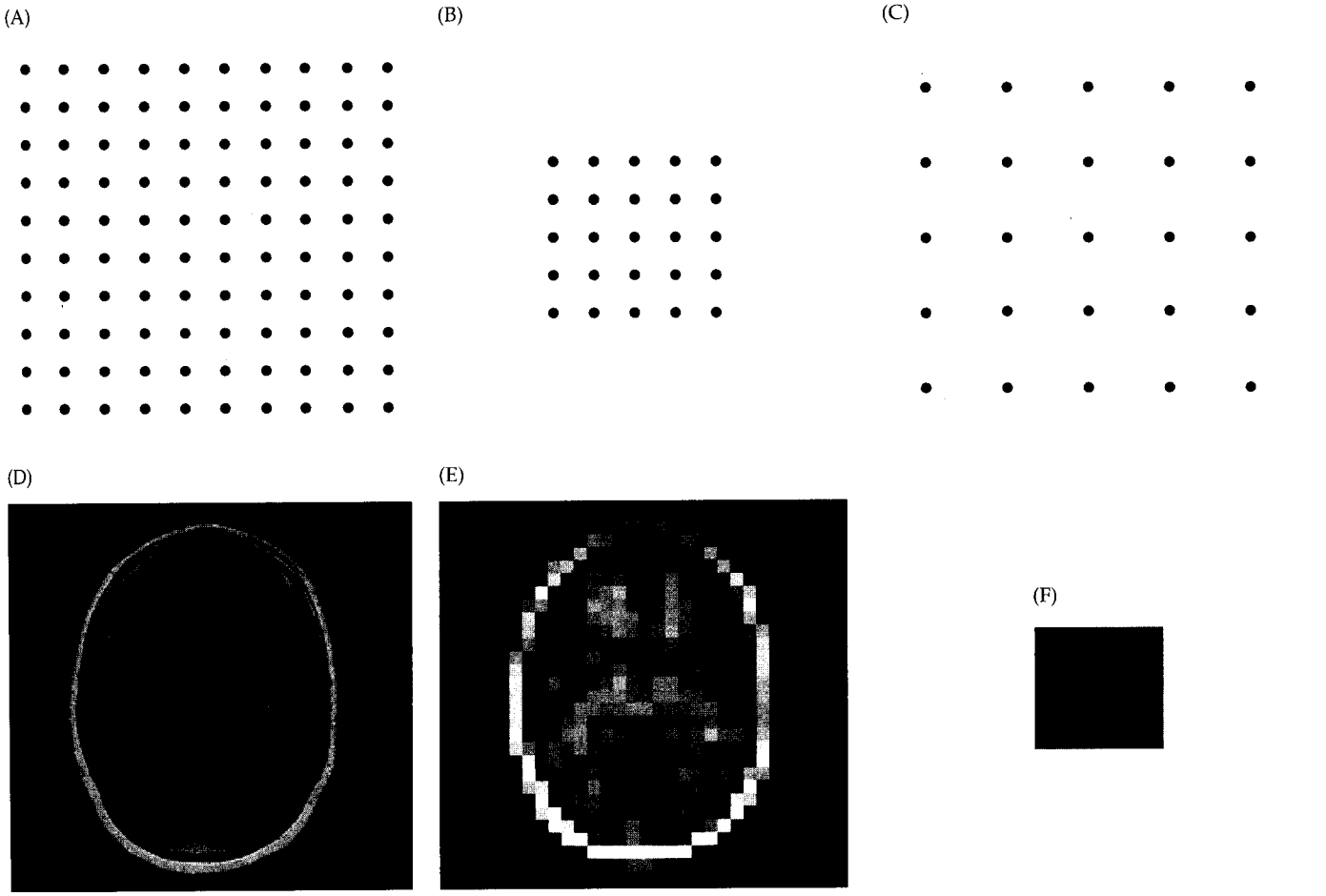

Figure 4.14 Effects of sampling in *k*-space upon the resulting images. Field of view and resolution have an inverse relation when applied to image space and *k*-space. (A) A schematic representation of densely sampled *k*-space with a wide field of view, resulting in the high-resolution image (D). (B) If only the center of *k*-space is sampled, albeit with the same sampling density, then the resulting image (E) has the same field of view but lower spatial resolution. (C) Conversely, if *k*-space is sampled across a wide field of view but with a limited sampling rate, the resulting image will have a small field of view but high resolution (F).

want to collect $N \times N$ voxels worth of data in our image, then we need an equal number of *k*-space data points ($N \times N$).

3-D Imaging

While 2-D imaging methods are common for most applications, not all MR imaging techniques are based on 2-D principles. Pulse sequences that collect *k*-space data in three dimensions are often used, especially for high-resolution anatomical images. Compared with 2-D imaging, 3-D sequences provide the primary advantage of a high signal-to-noise ratio, due to the fact that the 3-D volume can be larger than a single slice and therefore more excited spins can contribute to the MR signal. The principles of 3-D imaging can be easily extrapolated from those of 2-D imaging, so in theory any 2-D imaging sequence can be converted to 3-D. Since slice selection is unnecessary, the traditional slice excitation step is replaced by a volume excitation step that uses a very small *z*-gradient to select a thick slab. To resolve spatial

information along the z-direction, another phase-encoding gradient is presented along that dimension during the data acquisition phase. Therefore, within a typical 3-D pulse sequence, there are two phase-encoding gradients and one frequency-encoding gradient.

The concept of *k*-space can be expanded to three dimensions by adding k_z, defined by the time integral of the G_z gradient. To reconstruct the 3-D images, an inverse Fourier transform in three dimensions is executed. The following flowchart summarizes the steps of 3-D imaging:

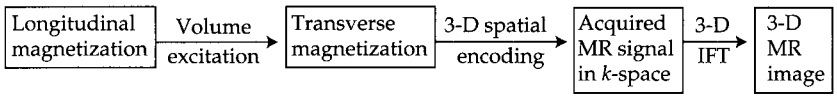

Unfortunately, the advantages of 3-D sequences are accompanied by several disadvantages. For example, the dimension of phase encoding usually is more vulnerable to field inhomogeneities and motion artifacts than the dimension of frequency encoding. Because 3-D imaging methods have two phase-encoding dimensions, they are more vulnerable to these artifacts. Also, more time is required to fill *k*-space when an entire volume is excited than when only a single slice is excited. Thus, movement of the head at any point within the acquisition window will cause distortions throughout the entire imaging volume. Within fMRI studies, 3-D imaging is typically restricted to anatomical scans, since the major classes of BOLD fMRI pulse sequences use 2-D methods.

Potential Problems in Image Formation

The goal of any image formation method is to achieve a true representation of the imaged object. Of course, in an ideal scanning environment with a perfectly uniform main magnetic field, exactly linear gradient fields, an absolutely square excitation profile, and optimized image acquisition software, there could be no problems! Under such perfect conditions, the acquired image will exactly match the scanned object in every way. It will be of the same size and shape, with local intensities dependent on the appropriate proton density and relaxation characteristics. Yet, as anyone with substantial MRI experience will attest, the images acquired under normal laboratory conditions are not always faithful to the original objects. We next consider some of the typical problems encountered in forming MR images.

The first problem to consider is inhomogeneity of the static magnetic field, meaning that the actual value of the field at one or more spatial locations is not the same as the theoretically desired quantity. Note that inhomogeneity of the static magnetic field across space becomes of increasing concern at higher field strengths, because it becomes more difficult to adequately shim the field to correct for local distortions. The imperfection in the static field can be mathematically represented by a difference quantity, ΔB_0, representing the increased or decreased field strength at a given location. Equation 4.22 is a modified version of the MR signal equation that contains the new term ΔB_0:

$$S(t) = \int_x \int_y m(x,y) e^{-i2\pi(k_x(t)x + k_y(t)y + \Delta B_0 t)} dxdy \qquad [4.22]$$

We usually do not know the exact nature of static field inhomogeneities, but if present they will introduce artifacts to images, following conventional

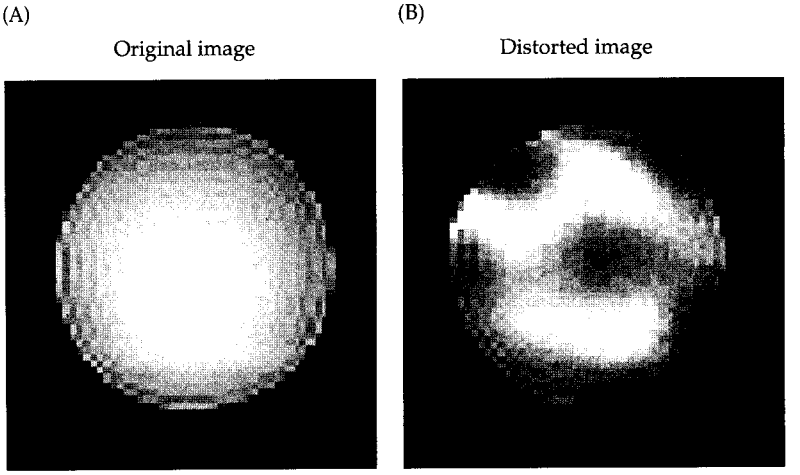

Figure 4.15 Spatial and intensity distortions due to magnetic field inhomogeneities. Under a homogeneous magnetic field, the image of a circular phantom is itself circular and of relatively similar intensity throughout (A). Local magnetic field inhomogeneities cause two types of distortions, geometric distortions and signal losses, both of which are visible on the distorted image (B).

inverse Fourier transformation. In practice, ΔB_0 can lead to two distinct types of artifacts: geometric distortions and variations in signal intensity. We can think of these artifact types, taken roughly, as macroscopic and microscopic effects.

Large-scale inhomogeneities cause geometric distortions due to spatial shifting of voxels. Because the frequency of spins depends upon the magnetic field strength, magnetic field inhomogeneities will lead to changes in spin frequencies. Remember from earlier in this chapter that the position of a voxel is encoded by its spin frequency. Thus, a voxel with the incorrect spin frequency will be displaced to an incorrect spatial location. Small-scale inhomogeneities cause spins within a voxel to lose coherence due to T_2^* effects. This reduces the total magnetization available within a voxel and thus reduces its signal intensity. These two effects may be present within the same image (Figure 4.15).

A second problem results from nonlinearities of the gradient fields. Because the spatial gradients control the *k*-space trajectories, we use *k*-space to evaluate their artifacts. Again, we consider a typical gradient-echo pulse sequence. First, if the *x*-gradient G_x is off by a small amount, as shown in Figure 4.16A, the resulting *k*-space trajectories will have an error along the k_x direction. Second, if the *y*-gradient G_y is off, the *k*-space trajectories will be skewed along the k_y direction (Figure 4.16B). Note that this skew affects both the onset of each line in *k*-space as well as the path taken through *k*-space. The magnitude of this skew depends on the time integral of the gradient amount. Third, if the *z*-gradient G_z is off, the slope of the excitation gradient will be altered. Altering the slope of the slice-selection gradient can compromise the match between the gradient-induced changes in spin frequency and the excitation pulse. However, because the *k*-space trajectory in the *x*–*y* plane would not change, the shape of the object would not be distorted. Thus, problems with the G_z gradient can lead to changes in slice thickness and signal intensity (Figure 4.16C).

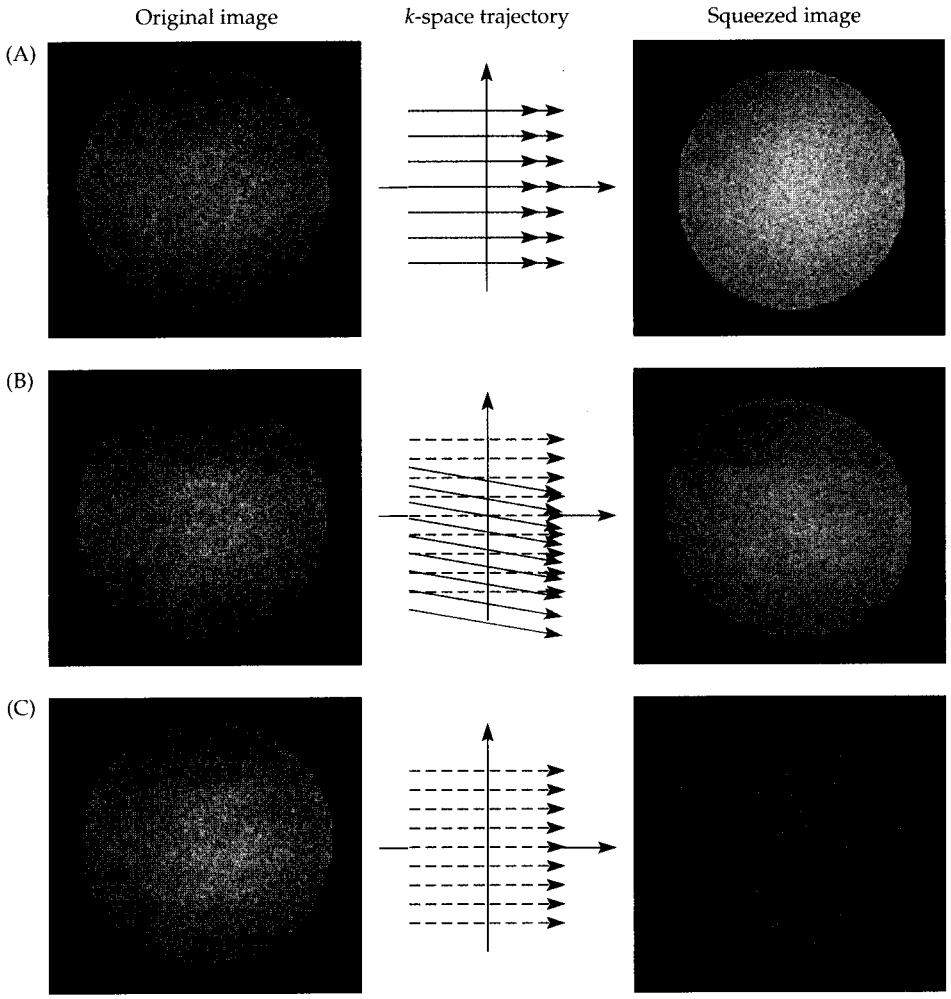

Figure 4.16 Image distortions caused by gradient problems. Each row shows the ideal image, the problem with acquisition in *k*-space, and the resulting distorted image. (A) Problems with the *x*-gradient will affect the length of the trajectory along the *x*-dimension in *k*-space, resulting in an image that appears compressed. (B) Problems with the *y*-gradient will affect the path taken through *k*-space over time, resulting in a skewed image. (C) Problems with the *z*-gradient will affect the match of excitation pulse and slice selection gradient, here resulting in a thinner slice and reduced signal intensity.

Summary

The net magnetization of a spin system, as described by the Bloch equation, can be broken down into separate spatial components along the *x*-, *y*-, and *z*-axes. By convention, the longitudinal magnetization is defined as $\mathbf{M_z}$ and the transverse magnetization is defined as $\mathbf{M_{xy}}$. The recovery of the longitudinal magnetization following excitation is governed by the time constant T_1, while the decay of the transverse magnetization following excitation is governed by the time constant T_2. The total MR signal measured is the combination of the transverse magnetization from all voxels in the sample and can be described using a single equation. The use of spatial gradients is necessary for measurement of spatial properties of a sample, in essence allowing MR to become MRI. The simultaneous application of a G_z gradient and an excitation pulse allows selection of a defined slice within the imaging volume. The use of two additional gradients within the slice allows unique encoding of spatial locations. Image acquisition can be considered using the concept of *k*-space, which reflects the Fourier transform of image space. Different pulse sequences sample *k*-space differently, and the inverse relation between sampling in *k*-space and sampling in image space is important to understand. Inhomogeneities in the magnetic field

experienced by spins can cause systematic artifacts in the reconstructed images, in the form of geometric distortions and signal loss.

Suggested Readings

Bracewell, R. N. (1986). *The Fourier Transform and Its Applications,* McGraw-Hill, New York. A textbook for everything you want to know (and more) about the Fourier transform.

Haacke, E. M., Brown, R. W., Thompson, M. R., and Venkatesan, R. (1999). *Magnetic Resonance Imaging: Physical Principles and Sequence Design,* John Wiley & Sons, New York. A comprehensive encyclopedia of the theoretical principles of MRI.

Twieg, D. B. (1983). The *k*-trajectory formulation of the NMR imaging process with applications in analysis and synthesis of imaging methods. *Med. Phys.,* 10(5): 610–621. An original description of the *k*-space trajectory formulation.